Marine Pollution Bulletin
November 2015, Volume 100, Issue 1, Pages 200-216
http://dx.doi.org/10.1016/j.marpolbul.2015.08.048
http://archimer.ifremer.fr/doc/00279/39050/

Informing Marine Spatial Planning (MSP) with numerical modelling: A case-study on shellfish aquaculture in Malpeque Bay (Eastern Canada)

Filgueira Ramón [1, *], Guyondet Thomas [1], Bacher Cedric [2], Comeau Luc A. [1]

[1] Department of Fisheries and Oceans, Gulf Fisheries Centre, Science Branch, P.O. Box 5030, Moncton, NB E1C 9B6, Canada
[2] French Institute for Sea Research (IFREMER), BP70, 29280 Plouzané, France

* Corresponding author : Ramón Filgueira, email address : ramonf@me.com

Abstract :

A moratorium on further bivalve leasing was established in 1999–2000 in Prince Edward Island (Canada). Recently, a marine spatial planning process was initiated explore potential mussel culture expansion in Malpeque Bay. This study focuses on the effects of a projected expansion scenario on productivity of existing leases and available suspended food resources. The aim is to provide a robust scientific assessment using available datasets and three modelling approaches ranging in complexity: (1) a connectivity analysis among culture areas; (2) a scenario analysis of organic seston dynamics based on a simplified biogeochemical model; and (3) a scenario analysis of phytoplankton dynamics based on an ecosystem model. These complementary approaches suggest (1) new leases can affect existing culture both through direct connectivity and through bay-scale effects driven by the overall increase in mussel biomass, and (2) a net reduction of phytoplankton within the bounds of its natural variation in the area.

Highlights

► Shellfish carrying capacity was explored using numerical modelling ► Scenario building was used to explore hypothetical aquaculture expansion ► Assessment for marine spatial planning was provided based on modelling outcomes

Keywords : Physical-biogeochemical model, Marine spatial planning, Aquaculture, Carrying capacity, Ecosystem-based management

1. Introduction

Mussel aquaculture is a significant industry in Prince Edward Island (PEI, Canada), with an annual production of approximately 20,000 tons (http://www.aquaculturepei.com, Statistics Canada 2010). The development of this farming activity in PEI started in the 1970s and has grown steadily in terms of production (Drapeau et al. 2006). Approximately 4500 ha of PEI estuarine waters are now leased out to individuals and companies for the specific purpose of cultivating mussels (Fisheries and Oceans Canada Charlottetown, hereafter DFO). In 1999, DFO instigated a moratorium on further leasing for mussel aquaculture in PEI. This moratorium was restricted to new applications, thereby allowing the leasing division to focus on backlog applications and assist with navigational and environmental assessments. In 2007, the Aquaculture Alliance of Prince Edward Island (Canada) made a formal request to DFO to review that moratorium. Malpeque Bay was identified as one of the last areas within the bays and estuaries of PEI for potential mussel culture expansion.

The total area of the Malpeque Bay system (Fig. 1a) is 19,640 ha of which 1,400 ha (~7%) are currently leased for aquaculture. In 2008, opportunities for further development of mussel aquaculture for food provision in Malpeque were examined by DFO. The conclusion was that lease expansion in Malpeque should be approached with caution, but an increase of aquaculture acreage in Malpeque from 7% up to 10% (an addition of 590 ha) was considered further. In 2013, DFO identified the need to develop a detailed spatial plan to accommodate this potential increase in aquaculture acreage taking into consideration other marine activities, aboriginal rights and stakeholder interests. The exact locations in the bay at which possible future mussel aquaculture leases could be considered, as well as areas in which aquaculture should be avoided because of conflict among marine users are still under consideration but one scenario was provided to DFO Science to guide in the assessment of carrying capacity. This projected scenario could be modified during subsequent steps of the consultation process and it has been considered in the present study because it is the only lease siting scenario provided.

In this study, the potential impact of future leases has been assessed under the umbrella of the well-known concept of Carrying Capacity (CC). The concept of CC is relatively new and started showing up in the bivalve literature in the 1980s. Four types of CC have been defined (Inglis et al. 2000, McKindsey et al. 2006): (1) Physical CC, which describes the area that is geographically available and physically/chemically adequate for a certain type of aquaculture; (2) Production CC, which is the optimized level of aquaculture production; (3) Ecological CC, which is defined as the magnitude of aquaculture production that can be supported without leading to unacceptable changes in ecological process, species, populations, or communities in the environment; and (4) Social CC, which can be defined as the amount of aquaculture that can be developed without adverse social impacts.

In regards to the Marine Spatial Planning (MSP) process in Malpeque, it could be said that exploratory analyses regarding physical, social and governance aspects of CC have been instigated over the past few years by DFO (unpublished). However, one aspect that remains unaddressed is the ecological CC. As ecosystem engineers, bivalves can exert multiple ecological impacts, such as (1) increasing the benthic loading of organic matter in the vicinity of the farms, which may in turn alter nutrient/oxygen fluxes and

benthic community composition (e.g. Giles and Pilditch 2006, McKindsey et al. 2011, McKindsey 2013), (2) depleting the water-column phytoplankton through intense grazing (e.g. Dame and Prins 1998, Newell 2004), (3) transferring diseases and hitchhiking species through stock movements (e.g. Forrest et al. 2009, Padilla et al. 2011), and (4) habitat creation/modification (e.g. McKindsey et al. 2011). The degree of most of these impacts depends on shellfish density and hydrodynamics (Mallet et al. 2006).

Given recent amendments to the Canadian Fisheries Act and a renewed emphasis on protecting the productivity of commercial, recreational and aboriginal (CRA) fisheries, one option for exploring ecological CC is focusing on phytoplankton abundance in the water column. Phytoplankton populations constitute the primary step in marine food webs and thus their preservation is an important tenet of ecosystem based management (Crowder and Norse 2008). Maintaining phytoplankton populations at a sustainable level should guarantee the flow of energy towards CRA species. A number of ecological CC frameworks based on the abundance of phytoplankton populations have been previously suggested for bivalve aquaculture sites (e.g. Bacher et al. 1998, Filgueira and Grant 2009). These frameworks necessarily involve computer modelling. Models integrate time and space, which is critical for understanding ecological dynamics and therefore how natural systems provide ecosystem services (Palmer et al. 2004). In addition, scenario building (~~-w~~hat if" scenarios) allows the exploration of future situations where unanticipated stressors generate new risks or opportunities, and is thus an important tool for managing those changes (Nobre et al. 2010).

In this study, three different modelling approaches have been applied to Malpeque Bay. The intent was to provide the most robust scientific assessment possible using available datasets. Specifically, the study was aimed at answering the following questions related to the MSP process:

- what is the current level of cultivated mussel biomass in Malpeque Bay?
- would increasing acreage by 590 ha impact the production of existing mussel farms?
- are there any indications that ecological capacity is already attained for some regions of Malpeque?

2. Material and methods

2.1. Study area and aquaculture practices

The Malpeque Bay system (Fig. 1a) is a large and shallow embayment located on the North shore of PEI. The bay is composed of several basins that cover a surface area of 223.6 km^2 for a total volume of 629.5 × 10^6 m^3. An intricate river system discharges into Malpeque at several different points. During the study period (May – October) individual river discharges are low, averaging between 0.29 and 0.55 m^3 s^{-1} (Environment Canada, http://www.ec.gc.ca). The system is open to the Gulf of St. Lawrence (GSL) through multiple connections. Tidal forcing is mainly diurnal and weak with an amplitude ranging from 0.15 m to 0.55 m from neap to spring tides. Given the low river discharge and weak tidal forcing, flushing of Malpeque Bay waters is rather slow. Renewal by GSL waters

takes from 5-10 d next to the inlets to 15-40 d in the main aquaculture areas and up to 75 d at the southern end of the bay (Bacher et al. submitted). Currently, most of the mussel aquaculture activity (blue polygons in Fig. 1a) is located in the Northeast area of the system in two sub-basins that are partially isolated from the main water body, Marchwater and Darnley Basin. Marchwater connectivity to the main water body is restricted by a series of islands and shallow areas (Fig. 1a). Darnley Basin is located close to the mouth of the bay and connected to the main system through a narrow channel (Fig. 1a). The other areas for mussel aquaculture are spread along the bay, emplaced in areas that are more open to circulation than Darnley Basin and Marchwater. The scenario examined in this study places the new leases in the central part of the system, South of Marchwater, and on the Western shore. These potential new leases are all at least 1500 feet (~457 m) from the shoreline and in waters at least 15 feet (~4.6 m) deep. The potential new leases would increase the aquaculture acreage in Malpeque from 7% to 10% of the spatial area of the bay.

Mussel aquaculture in PEI is carried out using a longline system of suspended polyethylene sleeves (Scarratt 2000). Seed collector ropes are deployed in spring and recovered in early autumn when recruited seed reach approximately 15—20 mm in shell length. Seed are stripped from collector ropes and placed into 1.8-m long polypropylene sleeves that hang from 100 to 200 m longlines, positioned 1 m below surface to avoid damage by a thick (~1 m) ice cover during winter. Sleeves are generally hung 44 cm apart along longlines, which in turn are moored 12 m apart (Drapeau et al. 2006). Mussels may attain a harvestable size (shell length > 55 mm) in the fall of their second year (~18 mo mussels), although most reach a harvestable size the following spring—summer (~24 mo mussels). Mussels are typically maintained at densities of between 1.10 and 2.07 kg per m^2 cultured area (Drapeau et al. 2006). Taking into account that approximately 58% of a lease area is utilized at any given time (Comeau et al. 2008), the effective density of mussels would range between 0.64 and 1.2 kg per m^2 of leased area.

2.2. Hydrodynamic model

A finite element model was developed for Malpeque Bay using the grid depicted in Fig. 1b and the RMA suite of models (Resource Modelling Associates, http://ikingrma.iinet.net.au). This model was used to reproduce water circulation within Malpeque Bay in response to tidal, meteorological (wind and atmospheric pressure) and river forcing. CTD vertical profiles (SBE-19plus, Sea-Bird Electronics, Bellevue, WA, USA) collected during summer-fall 2012 in conjunction with the water sampling described in Appendix A show no sign of long-term vertical stratification in temperature or salinity. Hence, a two-dimensional depth-averaged representation of the system is suitable to reproduce the main hydrodynamic features of Malpeque. The parameterization of the model does not include the effect of farming structures on hydrodynamics. Although bay-scale effects of farming structures are not expected given the generally good agreement between model and observations (Appendix B), local effects on water circulation cannot be discarded. Parameterization and calibration of the model was performed during summer-fall 2011 and is presented in Filgueira et al. (2014a) but also summarized in Appendix B. Once validated, the model was run under tidal and river forcing only. Meteorological data were not included because time series matching the period of time covered by the biogeochemical data (spring-fall 2012) were not available. The lack of meteorological forcing can reduce the mixing within the bay as discussed below. The outcomes of RMA were processed following Filgueira et al. (2012)

(See also Appendix C for a detailed description of the computation method) and were used in the connectivity and ecosystem analyses but not in the organic seston depletion analysis, which was performed using RMA.

The triangular mesh constructed for the hydrodynamic model, which contains 11,488 nodes and 5,171 elements (triangles), has been used in the three different modelling exercises carried out in this study. The current and future leases (Fig. 1a) were defined by selecting the nearest triangles in this mesh (Fig. 1b), which generates a bit of discrepancy in the shape of the leases. Nevertheless, the area that new leases occupy in the triangular mesh is 587 ha (Fig. 1b), which matches the projected expansion of 590 ha (Fig. 1a). The current leases were grouped and numbered from 101 to 107 and the future leases from 1001 to 1006 in order to facilitate the description of the results (Fig. 1b).

2.3. Connectivity analysis

Transfer time and transfer rate have been calculated using the outcomes of the hydrodynamic model in order to describe the spatial connectivity of the system. Transfer time (T_{ij}) from element j of the grid (Fig. 1b) to element i is defined as the average time taken to reach element i from element j. Transfer rate (R_{ij}) is the average percentage of matter that will reach element i in time T_{ij} when one unit of matter is released in element j at $t=0$. Computations of transfer time and transfer rate have been based on the algorithm developed by Leguerrier et al. (2006), which uses a matrix of probabilities, called a transition probability matrix, which summarizes the probability of a particle moving from one element to another during one time step. Such a matrix allows the identification of areas of the bay that are flushed and the time needed by particles to leave the bay. The main assumptions of this approach are i) the probability of finding the particle in any given element depends only on its location at the previous time, and ii) this probability does not change over time at some appropriate time scale. This is the basis of Markov Chain theory, with a considerable amount of literature dedicated to the analysis of the properties of such systems (e.g. Thompson et al. 2002). Leguerrier et al. (2006) have extended the application of this framework to the computation of ecosystem indicators – e.g. residence time, first passage time, rate of transfer, recycling index, and used these indicators to analyse preferential pathways of matter in a simplified food-web or physical system.

In this study, the transition probability matrix has been constructed using the average volumetric flows (m^3/d) among all pairs of adjacent elements calculated following Filgueira et al. (2012) (See Appendix C for a detailed description of the computation method). F_{ij} represents the flow going from element j to element i. The last column ($j = N+1$, where N is the number of elements in the grid) of the $F=(F_{ij})$ matrix corresponds to the inputs from the boundary, and the last row ($i = N+1$) to the outputs from the elements which are at the boundary. By definition, the total output from any element equals the total input to this element. The volume of element i is denoted V_i. The probability that a particle which is in element j at time t moves to element i during one time step Δt is equal to:

$$p_{ij} \quad — \qquad \text{for } i \in [1, N+1] \text{ and } j \in [1, N]$$

Probability for a particle that is in *i* to stay in *i* after one time step is given by:

$$p_{jj} \quad \sum_{\in} \quad p_{kj} \quad \text{for } j \in [1, N] \qquad \text{Eq. 2}$$

The transition probability matrix $\boldsymbol{P}=(p_{ij})$ can be used to simulate the evolution of a tracer concentration in time, from which residence and transfer times can be derived. However, Leguerrier's algorithm has several advantages. Without running simulations, it provides an efficient and quick way to estimate residence and transfer times for all elements at the same time. It also allows for the computation of other indicators – e.g. transfer rate, first passage time, etc. This is made possible by the properties of Markov Chain matrices and appropriate definitions of indicators. Following Leguerrier et al. (2006) transfer times T_{ij} and transfer rates R_{ij} from element *j* to element *i* for all (*i,j*) pairs have been computed. As an example, maps of transfer times and rates are displayed to show the results for one source element (Fig. 2). These indicators are then used to identify the main pathways of matter within the bay. For 2 elements *(i,j)*, it is considered that high R_{ij} and low T_{ij} correspond to a strong link between *j* and *i*, yielding a potential influence of *j* on *i*.

2.4. Organic seston depletion

The RMA11 module was used to define a suspended variable representing sestonic bivalve food. The dynamics of the seston are then reproduced by the convection-diffusion equation:

$$— \quad u\frac{P}{\partial x} + v\frac{P}{\partial y} \quad \overline{\partial x}\left(D_x\overline{\partial x}\right) + \overline{\partial y}\left(D_y\overline{\partial y}\right)$$

where *P* is the seston concentration in mgC m^{-3}, *u* and *v* are the current speeds in direction *x* and *y*, respectively, calculated by the hydrodynamic model, D_x and D_y are the dispersion coefficients proportional to *u* and *v*, respectively, α is the phytoplankton primary production rate in mgC m^{-3} d^{-1} and β is the bivalve population clearance rate in times per day. Therefore, seston renewal relies on both exchange with the far field and phytoplankton primary production within the bay. Other sources of seston, such as resuspension and inputs from terrestrial sources, were not included in the model. Terrestrial inputs are not expected to constitute a major source of seston during the summer period of low river discharge. On the other hand, resuspension might have an important influence on seston dynamics characterized by temporal and spatial heterogeneity due to episodic wind events and the dependence of wave action on wind direction and water depth. For simplicity and to focus on capturing the bivalve filtration signal, these processes were excluded from our analysis. Accordingly, organic seston concentration in this exercise should be understood as a theoretical tracer rather than an attempt to simulate the observed levels of seston within the bay. Therefore, the outcomes of the model should be interpreted in relative rather than in absolute terms, with the aim of identifying the most sensitive areas of the bay to bivalve aquaculture in terms of seston levels.

The primary production rate α was estimated from *in situ* measurements made during the summer of 2011 in Malpeque Bay (unpublished data) using the ^{14}C method (JGOFS

1994). Its value was kept uniform over the model domain and constant during the simulation period, and corresponded to a planktonic primary production rate of 65 gC m^{-2} yr^{-1}. No previous report of primary production rates in the area could be found. However, the value used here falls within observed rates for other estuaries in the region during the same 2011 campaign and sits at the lower end of the range (40-550 gC m^{-2} yr^{-1}) reported for temperate estuaries (Heip et al. 1995).

The bivalve population clearance rate β was calculated as the product of individual bivalve clearance rate (m^3 ind^{-1} d^{-1}) and density of bivalves in the farm area (ind m^{-2}) and divided by depth (m). Mussel density was adjusted according to the densities reported above, but an effective density was calculated by multiplying the reported densities by 0.88 assuming that mussels have their valves opened only 88 ± 2.1% of the time (Comeau et al. 2015). The model was populated with individuals of an average size of 45 mm shell length, and which filtered at a constant rate of 2.7 L h^{-1} (Comeau et al. 2015). This last term of Eq. 3 was only included in the model grid cells located inside the active farms. Two different scenarios with active farms were simulated, one with the current mussel leases and a second one with the current plus the potential projected leases (Fig. 1a).

In order to evaluate the net effect of transport, primary production and bivalve filtration on food availability, a Seston Depletion Index (SDI) was calculated from the model results. The SDI is expressed as a percent change in seston concentration relative to the boundary concentration (P_0) that was held constant during the simulations at a value P_0 = 1000 mgC m^{-3} corresponding to the mean of concentrations observed just outside Malpeque Bay between May and November 2012 (Guyondet et al., unpublished data, assuming 40% carbon content in the suspended particulate organic matter). To allow the seston concentration to reach an equilibrium state, the simulations are run for a period equal to or longer than the water renewal time of the area of interest. The concentration is then averaged over the last tidal cycle of the period at each node *n* of the model domain and this averaged concentration P_{avg} is compared to the boundary value to estimate the SDI as follows:

$$(n) \qquad \frac{(n)}{\qquad}$$

The SDI is sensitive to bivalve filtration. SDI < 0 denotes a decrease in seston availability due to bivalve filtration, whereas SDI > 0 reveals seston accumulation due to local primary production in less flushed areas.

2.5. Ecosystem analysis

The hydrodynamic model was coupled to a biogeochemical model constructed in Simile (http://www.simulistics.com) following Filgueira et al. (2012). The biogeochemical model (Table 1), which includes the submodels phytoplankton, nutrients, detritus and mussels, has been previously applied to Malpeque by Filgueira et al. (2014a). The latter paper provides a detailed explanation of the model equations, coupling, parameterization, forcing, calibration and validation. Mussel density was adjusted according to the densities stated earlier. The mussel submodel used in this study has been developed using Dynamic Energy Budget (DEB) Theory which has been validated worldwide (Rosland et al. 2009, Filgueira et al. 2011), including for other PEI embayments

(Filgueira et al. 2014b). Given that the DEB model that simulates mussel physiology adjusts the filtration activity according to environmental conditions, no further adjustments of effective density related to open/close behaviour were needed in this approach. Given that tunicates can play a significant role on phytoplankton populations, a phytoplankton mortality term was parameterized in the ecosystem model assuming that tunicates increase the filter-feeding capacity of cultured mussel operations by 15%. The solitary tunicate *Styela clava* is the most problematic fouler in Malpeque. The 15% estimate is based on an infestation level of 627 *S. clava* per sleeve and the implementation of control measures (liming) starting in August. At this time *S. clava* individuals are still relatively small (< 40 mm body length) and filter at a rate of approximately 0.6 l h^{-1} ind^{-1} (DFO, unpublished data). The fully-coupled model was run from 24 May 2012 to 7 October 2012 (137 days). The simulated period was determined by the availability of forcing data (see Appendix A for a detailed description of available forcing data). The same ecosystem model has been successfully applied to several bays in Atlantic Canada (Filgueira and Grant 2009; Filgueira et al. 2013a, 2014b, 2014c, 2014d). However, as reported by Filgueira et al. (2014a), the outcomes for Malpeque showed partial disagreement between field observations and predicted values. The lack of full validation increases the uncertainty of the model outcomes, which are discussed below.

In the same way as for the *'Organic seston depletion'* approach (section 2.4), two different scenarios were run, the first with the current mussel leases and the second with the current plus potential projected leases (Fig. 1a). In terms of output variables, a Phytoplankton Depletion Index (PDI) has been calculated following Eq. 4 and using chlorophyll as a proxy for phytoplankton abundance (chlorophyll time series at the boundary, see Appendix A, was used as P_0). In addition, in order to explore the sources of uncertainty in the model, a sensitivity test was performed for several parameters of the model. This analysis consisted in running different scenarios of the model by increasing/reducing a parameter +10/-10% and analyzing relative change of the outcomes in terms of nutrients, seston and chlorophyll concentration.

3. Results

3.1. Connectivity analysis

The main pathways of matter among leased areas have been identified analyzing transfer time (T_{ij}) and transfer rate (R_{ij}) from element *j* to element *i* for all the pairs of elements (*i*,*j*) that belong to any leased area. For example, the current leased area #101 is defined by 46 elements according to Fig. 1b and the projected leased area #1001 is defined by 41 elements; accordingly, 1886 (*i*,*j*) pairs (46×41) were calculated to evaluate the effect of leased area #101 on #1001. Similarly, 1886 (*i*,*j*) pairs were calculated to evaluate the effect of leased area #1001 on #101. The (*i*,*j*) pair of elements with a high connectivity, represented by a low T_{ij} and a high R_{ij}, were identified. Two different criteria were considered to identify (*i*,*j*) pairs with high connectivity: (1) T_{ij} < 20 days and R_{ij} > 10%, which suggests that the time that is required for a particle released in element *j* to reach element *i* is shorter than 20 days and the average amount of matter that reaches element *i* is above 10%; (2) T_{ij} < 10 days and R_{ij} > 50%. These thresholds are not based on any ecological process, and should be understood as two arbitrary criteria to identify connectivity among the leased areas. Given that the thresholds for the second criterion

are stricter than in the first one, the second criterion will identify the most significant connections among leased areas. For each criterion the number of (*i*,*j*) pairs that meet the thresholds were counted. After that, this number of successful connections for each leased area interaction, e.g. #101 on #1001, was divided by the total number of possible connections between the leased areas, e.g. 1886 for #101 on #1001, resulting in the percentage of connections between two leased areas. The results were compiled in frequency tables, Table 2 and 3 for $T_{ij} < 20$ & $R_{ij} > 10\%$ and $T_{ij} < 10$ & $R_{ij} > 50\%$ respectively.

The connectivity analysis for the $T_{ij} < 20$ & $R_{ij} > 10\%$ criterion is presented in Table 2. The diagonal of the table represents the intra-leased area connectivity, which is generally high, as expected. Only in small leased areas such as 105 can the currents minimize this connectivity. According to the values it appears that the current leases are not strongly connected to each other (upper left quadrant in Table 2). Only the connection between leased area #106 and #107 shows a strong 74% connectivity. On the contrary, the projected leases are subject to strong interactions to each other (bottom right quadrant in Table 2). The connectivity from projected leases to current leases (upper right quadrant in Table 2) is weak, with the highest connectivity from leased area #1006 to #103 with 25% of (*i*,*j*) pairs meeting the thresholds. It is important to highlight that leased area #101 from Darnley Basin, one of the most productive areas, is completely isolated from the projected leases, with 0% of successful connectivity. However, the connectivity from current leases to projected leases (bottom left quadrant in Table 2) is quite important, with the current leased areas affecting all the new projected leased areas to some degree. The most significant inter-lease connections, with percentage of connectivity > 40%, are represented in Figure 3. The most significant connections from current leases (represented in blue) to other leases are presented in Figure 3a. The outcome shows that current leases have an elevated potential of influencing projected leases (represented in red). The most significant connections from projected leases to other leases are presented in Figure 3b. While the projected leases are not significantly connected to the current leases, there is a strong connectivity among projected leases. Given that this probability analysis is based on the integration of large areas of the bay and ocean currents rather than Euclidean distances between areas, some of the results may appear unexpected when plotted in map view (Figure 3). For example, there is strong connectivity from lease #102 to #1001 (Figure 3a) but not from lease #102 to #105 (Figure 3a) even though #105 and #1001 are geographically close. The reason for this is that the connectivity from #102 to #1001 is only strong for the Northern part of #1001 but weak for the Southern part, where #1001 is close to #105 (Figure 3a).

The same analysis has been performed using the second criterion, $T_{ij} < 10$ & $R_{ij} > 50\%$ (Table 3). Given that the thresholds are more difficult to meet, this analysis only highlights the strongest connections. Similar conclusions can be extracted: low connectivity among current leases (upper left quadrant) and projected on current leases (upper right quadrant); but a higher connectivity from current leases to projected leases (bottom left quadrant) and particularly among the projected leases, which represent the highest connectivity according to this criterion (bottom right quadrant).

3.2. Organic seston depletion

The Seston Depletion Index (SDI) for the current lease scenario is presented in Figure 4a. Three main areas can be distinguished: (1) Darnley Basin (#101) and Marchwater (#102), in which the filtration pressure of mussel leases causes a maximum depletion up to -80% and -86% in Darnley Basin and Marchwater respectively; (2) the inner part of the Malpeque system, which is homogeneously enriched in organic seston compared to the values observed at the boundary; and (3) the main outer water body, near the opening of the embayment, which is slightly enriched in organic seston. This pattern suggests that the inner part of Malpeque is significantly enriched in organic seston and the enrichment gradually decreases towards the mouth of the bay due to dilution with the boundary. The presence of aquaculture, which is concentrated towards the mouth, reduces the organic seston in the outer part of the bay, consequently increasing the steepness of the inner-outer gradient.

A second scenario, which simultaneously included the current leases and the new projected leases, was simulated (Figure 4b). The projected leases are mostly located in the inner part of the bay that is enriched in seston under the current scenario (Figure 4a). The new leases shifted the SDI into a negative range (depletion) in most of the bay. Only the innermost areas of the bay, the heads of rivers and a small section protected by a barrier island in the Northwestern shore remained enriched in organic seston. It is noteworthy that the extent of depletion within the projected lease area is not as severe as in the existing lease areas. In other words the maximum depletion in the projected leases, -57%, is below the maximum value observed in current leases, -81% and -88% for Darnley Basin and Marchwater, respectively (Figure 4b). It is also noteworthy that the new leases would not amplify the depletion within the existing lease areas. The maximum depletion in Darnley Basin (~ -80%) and Marchwater (~ -90%) is similar in both scenarios (Figure 4a, b). Hence the projected leases would not affect the most sensitive areas, that is, the ones presently showing the lowest SDI.

The comparison of both current and projected scenarios in terms of changes in organic seston concentration is presented in Figure 5. In that figure, the organic seston concentration of the projected scenario has been subtracted from the current one, resulting in a map that highlights the areas that potentially would be more affected by the new leases in terms of seston depletion. The results show that the projected leases would not affect current mussel leases in Darnley Basin and the inner parts of Lennox (Northwest) and Marchwater. However, the projected leases would reduce organic seston concentration by a small extent (~0.2 mg C l^{-1}) over much of the Marchwater outer region, i.e., where the majority of existing leases in Marchwater are located and, as indicated earlier, depletion is already prominent. Projected leases would also reduce organic seston concentration in current leases located in the southern part of Malpeque, which is highly enriched in seston (see Figure 4a). In terms of magnitude, the most significant impact on current leases would occur within a small lease located on the Western shore (leased area #105), whose SDI would change from +50.3% in the current scenario (Figure 4a) to -40.5% in the projected scenario (Figure 4b), which represents a reduction in organic seston concentration of 0.9 mgC l^{-1} (Figure 5). This leased area is the closest one to the projected leases, only 400 m apart.

3.3. Ecosystem analysis

The Phytoplankton Depletion Index (PDI), an index analogous to SDI but exclusively for phytoplankton, has been calculated using the ecosystem model. In regards to the current leasing scenario (Figure 6a), PDI results show an enrichment of phytoplankton (PDI > 0) inside the bay compared to the phytoplankton levels at the boundary, highlighting the potential influence of river discharge on phytoplankton dynamics. Rivers, as important sources of nutrients, triggered steep gradients in chlorophyll concentration, with high values close the mouth that rapidly diluted downstream. The main water body of the system was quite homogeneous in terms of chlorophyll, and only the dense farming areas located in the northeast part of the bay substantially curtailed chlorophyll levels. The reduced enrichment and PDI at the mouth is consistent with the predicted SDI gradient (section 3.2). Figure 6b shows the PDI for the projected aquaculture scenario. Again there is consistency with the SDI in that the projected scenario curtails chlorophyll in most of the embayment. This effect can be seen as an extension of the lowest enriched area from the mouth of the bay towards the West and inner part of the system. Therefore both the SDI and PDI suggest bay-scale or ecosystem-scale effects associated to the projected leases. However, unlike the SDI, the PDI results suggest that current and projected aquaculture cannot deplete phytoplankton populations below boundary conditions.

At the bay-scale, the current aquaculture scenario reduces chlorophyll *a* by 0.3 µg l^{-1} compared to a scenario without aquaculture. In comparison, the current scenario + full projected lease scenario reduces chlorophyll *a* by 0.6 µg l^{-1}. A detailed representation of the absolute change in phytoplankton concentration is presented in Figure 7. The spatial pattern matches the one based on seston (Figure 5). It seems that the projected leases would reduce phytoplankton concentration over the entire system, but that the most substantial reduction would occur south of Courtin Island and extend into the Marchwater area. This reduction in phytoplankton concentration would therefore amplify the partial depletion already attributed to current leases in Marchwater. For that reason Marchwater would be the area most affected in terms of bivalve growth. In more detail, the ecosystem model suggests that projected leases would reduce mussel growth by 8±2% in the Marchwater area (s.d. values represent spatial variation), a value which is within the 20% variation of mussel growth typically measured for mussel culture in this area (Filgueira et al. 2013b). Similarly, the projected leases would lower mussel growth by 6% within the small lease on the Western shore (leased area #105). In comparison, only a 0.5% reduction in mussel growth is suggested for Darnley Basin.

The ecosystem model was also used to investigate whether a selective exclusion of projected leases could abolish or alleviate the impact on mussel growth in Marchwater. The projected leases closest to Marchwater (lease #1005 and #1006) were removed in the first simulation (Figure 8a), whereas projected lease #1003 was removed in the second simulation (Figure 8b). In both cases the bay became enriched in chlorophyll compared to the full projected scenario (Figure 6b). These changes were most apparent at the local scale in the vicinity of the excluded leases. At the ecosystem level both scenarios provided similar results. For example, when compared to a scenario without aquaculture, the bay-scale net reduction in chlorophyll *a* was 0.5 for both scenarios (#1005 and #1006 removed, and #1003 removed). Overall the two exclusion scenarios did not abolish the 8±2% impact on mussel growth forecasted above for Marchwater. However, the exclusion scenarios alleviated this impact, which fell to 7±2% (without #1003) and 4±1% (#1005 and #1006).

3.4. Sensitivity Tests

Table 4 summarizes the sensitivity tests carried out for several parameters of the ecosystem model. The analyses reveal that seston concentration is less sensitive to changes in the parameters than nutrients and chlorophyll concentration. Model outcomes are not very sensitive to changes in the parameters of the seston and mussel submodels that were evaluated. Three of the tested parameters caused changes in the model response greater than 10%, which suggests that the model is very sensitive to the calibration of these parameters. Remineralization rate caused a significant change in phytoplankton response, while phytoplankton mortality and changes in primary production affected both nutrient and chlorophyll concentration. Primary production rate was the parameter that most affected model outcomes, causing a change in phytoplankton concentration of +19.6% and -17.0% when the rate was changed +10% and -10%, respectively.

4. Discussion

4.1. Bivalve biomass in Malpeque

Estimates of cultivated mussel biomass are subject to uncertainty due to husbandry variables such as seeding densities, fall offs, and harvesting. Our calculations were based on leased area and husbandry information collected during other research projects (Drapeau et al. 2006, Comeau et al. 2008). We estimated the mussel biomass at 5120 to 9600 t. The wide range is attributable to the span of husbandry information reported by Drapeau et al. (2006) and Comeau et al. (2008). Interestingly, the estimate is consistent with a recent survey conducted in Malpeque (Monique Niles, DFO, unpublished data). During the summer of 2014, mussel longlines were counted and the total mussel biomass was estimated at 7039 t distributed amongst 926,212 sleeves. Considering that mussels are cultivated over a 2-year cycle, such standing stock or total biomass estimates are in broad agreement with the industry's reported 3430 t annual harvest (DFO Statistics). By comparison suspension cultured oyster biomass was estimated at only 367 t during the same survey in 2014. Bottom oyster biomass remains undocumented, rendering difficult a more comprehensive comparison between mussels and oysters. It is known however that the port landings of all oysters (cultured and wild confounded) averaged 169 t over the 1984—2011 period (DFO Statistics). The bulk of these oyster landings was located in (1) the Northwestern part of the bay, close to the open boundary with the Gulf of St. Lawrence, and (2) the Grand River area.

It is concluded that the cultured mussel is presently the dominant filter-feeder in Malpeque Bay. The opposite was likely true prior to the development of the mussel industry in the 1980s. Natural hard substrates for byssal attachment are scarce in PEI systems, and Malpeque oyster beds were presumably in better health before European colonization, habitat destruction, overfishing, and Malpeque disease (Bastien-Daigle et al. 2007, King and Burden 2009).

4.2. Impact of projected scenario on current leases and production carrying capacity

The calculations of transfer time and transfer rate following Leguerrier et al. (2006) provide a cost-effective analysis of the connectivity among different areas of a bay. The drawback of this approach is that the use of averaged water exchange coefficients accounts for the long-term circulation of the bay but not for high frequency events such as winds, which can increase mixing and trigger high frequency displacements of water within the bay. This drawback is aggravated by the lack of meteorological forcing due to the lack of appropriate time series data. Therefore, high frequency forcing was not accounted for, which can result in an underestimation of the mixing within the bay. Accordingly, while the application of average dynamics is useful for looking at long term effects such as growth, it is less appropriate for assessing the risk of disease transfer or non-native species distribution, both of which can be affected by high frequency forcing. Consequently, the connectivity approach should be understood as a probabilistic and relative analysis that aims to identify the strongest spatial connections rather than an accurate description of the circulation of the bay.

The use of different thresholds of transfer time and transfer rate allows the identification of areas with strongest connectivity. The results of these analyses highlights that the effects of projected leases on current leases are relatively less important than the effects of current leases on projected leases and current leases among themselves (Table 2 and 3, Figure 3). Accordingly, it seems that the effects of the new projected leases on current leases result from global (bay-scale) dynamics rather than a direct interaction.

Special attention was directed towards Marchwater. The mussel industry is particularly concerned that the projected leases will reduce growing conditions in this area. It is reasoned that a reduction in the availability of suspended food particles could reduce the production of current leases and consequently decrease the value of these leases. The results of this study suggest that projected leases would reduce mussel growth by 8±2% in the Marchwater area during the study period. A selective exclusion of projected leases reduced the impact from 8±2% to 7±2% or 4±1%, removing lease #1003 and leases #1005-1006 respectively. Therefore the impact was not completely eliminated by excluding the future development closest to Marchwater. Obviously, removing the closest leases to Marchwater, #1005 and #1006, triggered the highest improvement, but removing lease #1003 also caused positive effects, suggesting that bay-scale effects related to a global increase in bivalve biomass are also important.

In term of production CC, mussel landings in Malpeque averaged 3,431 t annually between 2000 and 2011 (DFO Statistics). A back-of-the-envelope calculation suggests that an additional 590 ha would yield another 2,629 t annually, representing by itself a landed value of $3.5M/year. We caution that these estimates do not take into account possible extensions of the production cycle or reduced meat contents due to increased competition for food particles.

4.3. Ecological carrying capacity

The analysis of ecological CC focused on cultured mussels and their impact on suspended food resources, namely seston and phytoplankton. First, the seston depletion index (SDI) was based on a hydrodynamic model representing the dynamics of organic

seston in coastal waters (Guyondet et al. 2013). The simplification of the model from the biogeochemical perspective provides advantages and disadvantages. The model is easy to parameterize but the SDI absolute values cannot represent the actual variation in seston concentration. The SDI must rather be seen as a relative criterion allowing the identification of potentially sensitive areas (Guyondet et al. 2013). The second methodological approach relating to the phytoplankton depletion index (PDI) increases complexity in an attempt to bolster ecological realism. Admittedly, imperfect knowledge of ecological relationships, parameters and forcing functions may also lead to greater scientific uncertainty (FAO 2008). This implies that modelling should restrict its focus to relevant components and critical dynamics, which must be defined based on the management question to be addressed, available data (including forcing conditions), the important system features and the appropriate scales (FAO 2008, Fulton 2010). The information for constructing an ecosystem model based on a nutrient-phytoplankton-zooplankton model with the addition of mussel and seston submodels was available for Malpeque. However, the ecosystem model showed partial disagreement between field observations and predicted values, which mainly were related to an overestimation of simulated phytoplankton concentration (Filgueira et al. 2014a). The potential causes of this overestimation are discussed in Filgueira et al. (2014a) but in summary are related to (1) the uncertainty in discharge of nutrients from rivers; (2) the use of certain parameters [remineralization, primary productivity and phytoplankton mortality] measured in neighbouring PEI bays but identified as very sensitive parameters (Table 4); (3) the fact that phytoplankton productivity in the model is limited by nitrogen, which is possibly not the case for Malpeque according to Meeuwig et al. (1998), since turbidity and the adsorption of phosphorous to the iron-rich soils of PEI may cause light and phosphorous to be limiting factors; (4) the lack of other primary producers such as eelgrass and especially *Ulva* sp., which could play an important role in productivity and nutrient dynamics in PEI embayments (Raymond et al. 2002; Bugden et al. 2014); and (5) the lack of winds and waves on hydrodynamic forcing, which could result in an underestimation of mixing within the bay. The lack of winds is a consequence of the absence of field data to parameterize and validate the model during the period in which biogeochemical data was collected. The underestimation of mixing represents the worst-case scenario for local depletion of phytoplankton and consequently for mussel growth. Therefore, removing high frequency forcing provides a more precautionary approach to food dynamics and carrying capacity. Further research on these topics would provide positive feedback to the ecosystem model, improving its forecasting capabilities.

Given the SDI's conceptual limitations and the PDI's uncertainties, the present study cannot provide a definitive assessment of ecological CC in Malpeque. However, this conclusion does not invalidate the usefulness of the study for the MSP process. In the field of applied sciences, researchers and managers must be able to make objective decisions without full knowledge, but by using fully what is known at the time (Polasky et al. 2011). According to this philosophy, the best prediction based on current knowledge of the Malpeque system suggests that the full expansion of aquaculture would lower bay-scale chlorophyll *a* levels by 0.6 µg l^{-1} compared to a hypothetical scenario without aquaculture. This reduction is within the range of natural variability within the bay (3.0±1.1 µg l^{-1}, from Filgueira et al. 2014a), which has been suggested as a criterion for ecological carrying capacity (Grant and Filgueira 2011). Keeping phytoplankton reduction within its range of natural variability suggests that aquaculture signals on phytoplankton dynamics cannot be detected against the ecosystem background noise (Ferreira et al. 2013). In percentages, this change in chlorophyll represents a decrease of 17.7% compared to a hypothetical scenario without aquaculture. This reduction is

below the 20-30% observed in St. Peter's Bay (Guyondet et al. *in press*), a system that has reached its carrying capacity. Despite the fact that the reduction in chlorophyll in the projected scenario is below a neighboring embayment further research is needed to objectively define thresholds for ecological CC in Malpeque. The definition of objective thresholds for ecological CC is still in its infancy worldwide and the challenge lies in quantifying the limit at which changes in ecological processes are considered unacceptable (Duarte et al. 2003, Fisher et al. 2009). Soto et al. (2008) framed this topic in terms of resilience by stating that aquaculture should be developed in the context of ecosystem functions and services with no degradation of these beyond their resilience capacity. According to this approach, Grant and Filgueira (2011) have defined objective precautionary thresholds of ecological CC based on the reduction of chlorophyll concentration caused by cultured bivalves and the natural variability of phytoplankton biomass at the far field. These thresholds are based on the premise that cultivated bivalves should not be allowed to graze primary producers down to a level outside their natural variability range, which is assumed to be close to the tipping points of resilience. Consequently, further research is needed not only to improve forecasting capabilities but also to understand the resilience of the system, with emphasis on phytoplankton dynamics.

4.4. Conclusions

In this study, three complementary modelling approaches with different levels of complexity have been used to explore the connectivity among mussel leases and the ecological carrying capacity of a future aquaculture scenario for the Malpeque system. The connectivity analysis accounts for the physics alone, SDI combines physics and some basic ecology, and finally, PDI describes a simplified version of the ecosystem. In regards to the full projected scenario, consisting of an additional 590 ha of mussel leases, the analysis indicated (1) a 8±2% reduction in mussel growth in the Marchwater area due in part to direct connectivity among leases but also to bay-scale effects driven by the overall increase in bivalve biomass within the bay, and (2) a net reduction of chlorophyll *a* of 17.7% at the bay-scale compared to a hypothetical scenario without aquaculture. Sensitivity tests allowed the identification of key processes that should be studied in further steps in order to improve forecasting capabilities. This cautionary note is consistent with the concept of MSP, which is a dynamic process allowing feedback within a context of adaptive management (Halpern et al. 2011, Polasky et al. 2011). Adaptive management constitutes a structured and iterative decision making process that includes uncertainty; it aims to reduce uncertainty by incorporating feedback generated by monitoring programs. The model outcomes should be understood as the best objective scientific assessment that is presently possible with the available data and siting information. Therefore, regarding the MSP process, this study delivers objective scientific predictions (chlorophyll and bivalve growth), thresholds to interpret these predictions (based on natural variation of ecosystem variables), as well as a detailed analysis of uncertainty in the context of adaptive management. Consequently, this information could be used to inform marine spatial planning and decision makers on the role of the aquaculture expansion at the ecosystem level.

Acknowledgements

This research was funded by the Canadian Department of Fisheries and Oceans under the Program for Aquaculture Regulatory Research (Project PARR-2011-G-04). The authors gratefully acknowledge Lori Cuddy, Michael Cherry and Thomas Landry for helpful discussions. Michel Starr and Liliane St-Amand generously provided their expertise on primary production measurements. Thanks are also due to Rémi Sonier, André Nadeau and Tina Sonier for laborious field and laboratory work.

References

Bacher C, Duarte P, Ferreira JG, Héral M, Raillard O (1998) Assessment and comparison of the Marennes–Oléron Bay (France) and Carlingford Lough (Ireland) carrying capacity with ecosystem models. Aquat Ecol 31(4):379–394

Bacher C, Filgueira R, Guyondet T. Probabilistic approach of water residence time and connectivity using Markov Chains with application to tidal embayments. Submitted to Journal of Marine Systems

Bastien-Daigle S, Hardy M, Robichaud G (2007) Habitat management qualitative risk assessment: water column oyster aquaculture in New Brunswick. Can Tech Rep Fish Aquat Sci 2728: vii + 72 p

Bugden G, Jiang Y, van den Heuvel MR, Vandermeulen H, MacQuarrie KTB, Crane CJ, Raymond BG (2014) Nitrogen Loading Criteria for Estuaries in Prince Edward Island. Can Tech Rep Fish Aquat Sci 3066: vii + 43p

Byron CJ, Costa-Pierce BA (2013) Carrying capacity tools for use in the implementation of an ecosystems approach to aquaculture. In: Ross LG, Telfer TC, Falconer L, Soto D, Aguilar-Manjarrez J (eds) Site selection and carrying capacities for inland and coastal aquaculture. FAO/Institute of Aquaculture, University of Stirling, FAO Fisheries and Aquaculture Proceedings No. 21, Rome, pp 87–101

Comeau LA, Drapeau A, Landry T, Davidson J (2008) Development of longline mussel farming and the influence of sleeve spacing in Prince Edward Island Canada. Aquaculture 281:56–62

Comeau, L. A., R. Filgueira, T. Guyondet, and R. Sonier. 2015. The impact of invasive tunicates on the demand for phytoplankton in longline mussel farms. Aquaculture http://dx.doi.org/10.1016/j.aquaculture.2015.02.018

Crowder L, Norse E (2008) Essential ecological insights for marine ecosystem-based management and marine spatial planning. Mar Policy 32:772-778

Dame RF, Prins TC (1998) Bivalve carrying capacity in coastal ecosystems. Aquat Ecol 31:409-421

Drapeau A, Comeau LA, Landry T, Stryhn H, Davidson J (2006) Association between longline design and mussel productivity in Prince Edward Island, Canada. Aquaculture 261:879-889

Duarte P, Meneses R, Hawkins AJS, Zhu M, Fang J, Grant J (2003) Mathematical modelling to assess the carrying capacity for multi-species culture within coastal waters. Ecol Model 168:109-143

FAO (2008) Fisheries Management. 2. The ecosystem approach to fisheries. 2.1 Best practices in ecosystem modelling for informing an ecosystem approach to fisheries. Technical guidelines for responsible fisheries 4. Suppl. 2 Add 1. FAO, Rome

Ferreira JG, Grant J, Verner-Jeffreys DW, Taylor NGH (2013). Carrying Capacity for Aquaculture, Modeling Frameworks for Determination of. In: Christou P, Savin R, Costa-Pierce B, Misztal I, Whitelaw B (eds) Sustainable Food Production, Springer, Science+Business Media New York DOI 10.1007/978-1-4614-5797-8, pp 417-448

Filgueira R, Grant J (2009) A box model for ecosystem-level management of mussel culture carrying capacity in a coastal bay. Ecosystems 12:1222-1233

Filgueira R, Rosland R, Grant J (2011) A comparison of Scope For Growth (SFG) and Dynamic Energy Budget (DEB) models applied to the blue mussel (*Mytilus edulis*). J Sea Res 66:403-410

Filgueira R, Grant J, Bacher C, Carreau M (2012) A physical-biogeochemical coupling scheme for modeling marine coastal ecosystems. Ecol Inform 7:71-80

Filgueira R, Grant J, Stuart R, Brown MS (2013a) Operational models for Ecosystem-Based Management of bivalve aquaculture sites in data-poor environments. Aquacult Environ Interact 4:117-133

Filgueira R, Comeau LA, Landry T, Grant J, Guyondet T, Mallet A (2013) Bivalve condition index as an indicator of aquaculture intensity: a meta-analysis. Ecol Indic 25:215-229

Filgueira R, Guyondet T, Comeau LA (2014a) Preliminary carrying capacity analysis of current and future aquaculture scenarios in Malpeque Bay (Prince Edward Island) Can. Tech. Rep. Fish. Aquat. Sci. 3081: vii + 28 p

Filgueira R, Guyondet T, Comeau LA, Grant J (2014b) Physiological indices as indicators of ecosystem status in shellfish aquaculture sites. Ecol Indic 39:134-143

Filgueira R, Grant J, Strand Ø (2014c) Implementation of marine spatial planning in shellfish aquaculture management: modelling studies in a Norwegian fjord. Ecol Appl 24(4):832-843

Filgueira R, Guyondet T, Comeau LA, Grant J (2014d) A fully-spatial ecosystem-DEB model of oyster (*Crassostrea virginica*) carrying capacity in the Richibucto Estuary, Eastern Canada. J Mar Syst 136:42-54

Fisher J, Peterson GD, Gardner TA, Gordon LJ, Fazey I, Elmqvist T, Felton A, Folke C, Dovers S (2009) Integrating resilience thinking and optimization for conservation. Trends Ecol Evol 24(10):549-554

Forrest BM, Keeley NB, Hopkins GA, Webb SC, Clement DM (2009) Bivalve aquaculture in estuaries: review and synthesis of oyster cultivation effects. Aquaculture 298:1–15

Fulton EA (2010) Approaches to end-to-end ecosystem models. J Mar Syst 81:171-183

Giles H, Pilditch CA (2006) Effects of mussel (*Perna canaliculus*) biodeposit decomposition on benthic respiration and nutrient fluxes. Mar Biol 150(2): 261–271

Grant J, Filgueira R (2011) The application of dynamic modelling to prediction of production carrying capacity in shellfish farming. In: Shumway SE (ed) Aquaculture and the environment. Wiley-Blackwell, Chichester, pp 135−154

Guyondet T, Sonier R, Comeau LA (2013) A spatially explicit seston depletion index to optimize shellfish culture. Aquacult Environ Interact 4:175-186

Guyondet T, Comeau LA, Bacher C, Grant J, Rosland R, Sonier R, Filgueira R. Climate change increases carrying capacity in a coastal embayment dedicated to shellfish aquaculture. Estuar Coast *In press*

Halpern BS, Diamond J, Gaines S, Gelcich S, Gleason M, Jennings S, Lester S, Mace A, McCook L, McLeod K, Napoli N, Rawson K, Rice J, Rosenberg A, Ruckelshaus M, Saier B, Sandifer P, Scholz A, Zivian A (2011) Near-term priorities for science, policy and practice of Coastal and Marine Spatial Planning (CMSP). Mar Policy 36:198-205

Heip CHR, Goosen NK, Herman PMJ, Kromkamp J, Middelburg L, Soetaert K (1995) Production and consumption of biological particles in temperate tidal estuaries. Ann Rev Ocean Mar Biol 33:1-149

Inglis GJ, Hayden BJ, Ross AH (2000) An Overview of Factors Affecting the Carrying Capacity of Coastal Embayments for Mussel Culture. NIWA, Christchurch. Client Report CHC00/69: vi+31 p

JGOFS (1994) Primary production by 14C. In: UNESCO (ed) Protocols for the joint global ocean flux study (JGOFS) core measurements, Intergovernmental Oceanographic Commission Manual and Guides no 29, p 128-135

King, B. and Burden PJ 2009/ History of the Malpeque Oyster. The PEI Shellfish Association. ISBN 978-0-9684101-4-8

Leguerrier D, Bacher C, Benoît E, Niquil N (2006) A probabilistic approach of flow-balanced network based on Markov chains. Ecol Model 193:295-314

McKindsey CW, Thetmeyer H, Landry T, Silvert W (2006) Review of recent carrying capacity models for bivalve culture and recommendations for research and management. Aquaculture 261(2):451–462

McKindsey CW, Archambault P, Callier MD, Olivier F (2011) Influence of suspended and off-bottom mussel culture on the sea bottom and benthic habitats: a review. Can J Zool 89:622–646.

McKindsey CW (2013) Carrying capacity for sustainable bivalve aquacutlure. In: Christou P, Savin R, Costa-Pierce B, Misztal I, Whitelaw B (eds) Sustainable Food Production, Springer, Science+Business Media New York DOI 10.1007/978-1-4614-5797-8, pp 449-466

Meeuwig JJ, Rasmussen JB, Peters RH (1998) Turbid waters and clarifying mussels: their moderation of empirical chl:nutrient relations in estuaries in Prince Edward Island, Canada. Mar Ecol Prog Ser 171:139-150

Newell RIE (2004) Ecosystem influences of natural and cultivated populations of suspension-feeding bivalve molluscs: a review. J Shellfish Res 23:51–61

Nobre AM, Ferreira JG, Nunes JP, Yan X, Bricker S, Corner R, Groom S, Gu H, Hawkins A, Hutson R, Lan D, Lencart e Silva JD, Pascoe P, Telfer T, Zhang X, Zhu M (2010) Assessment of coastal management options by means of multilayered ecosystem models. Estuar Coast Shelf Sci 87:43–62

Padilla DK, McCann MJ, Shumway SE (2011) Marine invaders and bivalve aquaculture: sources, impacts and consequences. In: Shumway SE (ed) Aquaculture and the environment. Wiley-Blackwell, Chichester, pp 395−424

Palmer M, Bernhardt E, Chornesky E, Collins S, Dobson A, Duke C, Gold B, Jacobson R, Kingsland S, Kranz R, Mappin M, Martinez ML, Micheli F, Morse J, Pace M, Pascual M, Palumbi S, Reichman OJ, Simons A, Townsend A, Turner M (2004) Ecology for a crowded planet. Science 304:1251-1252.

Polasky S, Carpenter SR, Folke C, Keeler B (2011) Decision-making under great uncertainty: environmental management in an era of global change. Trends Ecol Evol 26(8):398-404

Raymond BG, Crane CS, Cairns DK (2002) Nutrient and chlorophyll trends in Prince Edward Island estuaries. In Effects of Land Use Practices on Fish, Shellfish and Their Habitats on Prince Edward Island. Edited by D.K. Cairns. Can Tech Rep Fish Aquat Sci 2408. pp 142-153

Rosland R, Strand Ø, Alunno-Bruscia M, Bacher C, Strohmeier T (2009) Applying Dynamic Energy Budget (DEB) theory to simulate growth and bio-energetics of blue mussels under low seston conditions. J Sea Res 62:49-61

Scarratt DJ (2000) Development of the mussel industry in western Canada. Bull Aquacult Assoc Can 100:37-40

Soto D, Aguilar-Manjarrez J, Brugère C, Angel D, Bailey C, Black K, Edwards P, Costa-Pierce B, Chopin T, Deudero S, Freeman S, Hambrey J, Hishamunda N, Knowler D, Silvert W, Marba N, Mathe S, Norambuena R, Simard F, Tett P, Troell M, Wainberg A

(2008) Applying an ecosystem based approach to aquaculture: principles, scales and some management measures. In: Soto D, Aguilar-Manjarrez J, Hishamunda N (eds) Building an ecosystem approach to aquaculture. FAO/Universitat de les Illes Balears Expert Workshop. 7–11 May 2007, Palma de Mallorca, Spain. FAO Fisheries and Aquaculture Proceedings. No. 14. Rome, FAO. pp 15–35.

Statistics Canada (2010) Aquaculture Statistics. (Catalogue no. 23-222-X). http://www.aquaculture.ca/files/documents/StatsCanAquacultureData2010.pdf

Thompson KR, Dowd M, Shen Y, Greenberg DA (2002) Probabilistic characterization of tidal mixing in a coastal embayment: a Markov Chain approach. Cont Shel Res 22:1603-1614

Tables

Table 1. Ecosystem model equations and terms.

Ecosystem model equations		
$$\frac{dP}{dt} = +P_{growth} - P_{mortality} - M_{grazing} \pm P_{mixing}$$		
$$\frac{dN}{dt} = +N_{river} + D_{remineralization} + M_{excretion} - P_{uptake} \pm N_{mixing}$$		
$$\frac{dD}{dt} = +D_{resuspension} + M_{feces} + P_{mortality} - D_{sinking} - D_{remineralization} \pm D_{mixing}$$		
$$\frac{dM}{dt} = +M_{grazing} - M_{excretion} - M_{feces}$$		
Term	**Definition**	**Reference**
dP/dt	Phytoplantkton change rate (mgC m^{-3} d^{-1})	
P_{growth}	Phytoplankton growth	
$P_{mortality}$	Phytoplankton mortality	Eq. 7 in Grant et al. (2007)
$M_{grazing}$	Mussel grazing on phytoplankton	
P_{mixing}	Exchange of phytoplankton with adjacent elements and/or far field	
dN/dt	Nitrogen change rate (mgN m^{-3} d^{-1})	
N_{river}	Nitrogen river discharge	River discharge x River Nitrogen concentration
$D_{remineralization}$	Detritus reminiralization	See Dowd (2005)
$M_{excretion}$	Mussel nitrogen excretion	Eq. 17 in Grant et al. (2007)
P_{uptake}	Phytoplankton nitrogen uptake	Eq. 15 in Grant et al. (2007)
N_{mixing}	Exchange of nitrogen with adjacent elements and/or far field	
dD/dt	Detritus change rate (mgC m^{-3} d^{-1})	
$D_{resuspension}$	Detritus resuspension forced by wind	Filgueira and Grant (2009)
M_{feces}	Mussel feces production	Eq. 5 in Grant et al. (2007)
$P_{mortality}$	Phytoplankton mortality	See above
$D_{sinking}$	Detritus removal by sinking	Eq. 5 in Grant et al. (2007)
$D_{remineralization}$	Detritus remineralization	See text
D_{mixing}	Exchange of detritus with adjacent elements	
dM/dt	Mussel change rate (mgC m^{-3} d^{-1})	
$M_{grazing}$	Mussel grazing on phytoplankton	DEB model (Rosland et al. 2009, Filgueira et al. 2011)
$M_{excretion}$	Mussel nitrogen excretion	
M_{feces}	Mussel feces production	

Table 2. Percentage of connections among leased areas that meet the criterion: Transit time < 20 days and transfer rate > 10%. Italic values: intra-lease connectivity. Bold values: The most significant inter-lease connections (percentage of connectivity > 40%).

Particles arriving in lease \ Particles originating from lease	101	102	103	104	105	106	107	1001	1002	1003	1004	1005	1006
101	*89*	7											
102	4	*54*								1		5	
103			*50*										25
104				*73*									
105					*33*	9		19					
106						*65*	**74**	4					
107						**74**	*50*	2					
1001	3	**49**			**67**	**52**		*74*	32	**44**	24	3	3
1002					**100**	13		**91**	*56*	4			
1003	2	39			**81**	19		**81**	**90**	*89*	**93**	**40**	15
1004	4	**45**		12	**77**	28		**78**	**86**	**92**	*88*	**56**	**41**
1005			15	**56**		5	6	6	15	**46**	**69**	*81*	**85**
1006			**45**	**76**	27	1		36	**70**	**70**	**73**	**94**	*90*

Table 3. Percentage of connections among leased areas that meet the criterion: Transit time < 10 days and transfer rate > 50%. Italic values: intra-lease connectivity.

Particles arriving in lease \ Particles originating from lease	101	102	103	104	105	106	107	1001	1002	1003	1004	1005	1006
101	*59*	3											
102		*19*											
103			*50*										
104				*39*									
105					*22*	4							
106						*45*	17	1					
107							*50*						
1001					22	3		*25*	1	1	3		
1002									*38*				
1003					4	<1		9	15	*46*	25		
1004					15	<1		22	38	23	*39*	1	
1005											2	*35*	18
1006				11							6	13	*46*

Table 4. Sensitivity test for different parameters of the ecosystem model. The effect of changing a parameter has been evaluated in three different components of the model, nutrient, seston and chlorophyll concentration.

Sub-model	Parameter	Change (%)	Nutrients (%)	Seston (%)	Chl-a (%)
Nutrients	Nutrient discharge	10	0.1	1.3	2.5
		-10	-0.1	-1.3	-2.5
	Remineralization	10	1.6	6.8	**14.4**
		-10	-2.1	-6.1	**-12.7**
Phytoplankton	Primary Production	10	**-13.6**	9.7	**19.6**
		-10	**17.7**	-8.5	**-17.0**
	Phytoplankton mortality	10	**14.4**	1.0	-7.4
		-10	**-12.9**	-1.3	8.4
Seston	Sinking and burial rates	10	-0.4	-5.7	-4.3
		-10	0.4	6.3	4.5
	J to mgC	10	-1.9	0.3	0.9
		-10	2.5	-0.4	-1.1
Mussel	X_K	10	-0.7	0.1	0.4
		-10	0.8	-0.2	-0.4
	$\{\dot{p}_{\mathrm{Xm}}\}$	10	2.1	-0.4	-1.1
		-10	-2.0	0.5	1.2
	$[\dot{p}_{\mathrm{M}}]$	10	0.1	0.1	0.2
		-10	-0.1	-0.1	-0.2

Figures

Figure 1. A. Water depth, current and new mussel leases (blue and red polygons respectively), as well as oyster leases (dark red). B. Triangular mesh used in the modelling exercises and current and future mussel cultivation areas, blue and red, respectively. Cultivation areas have been coded to facilitate the description of the results.

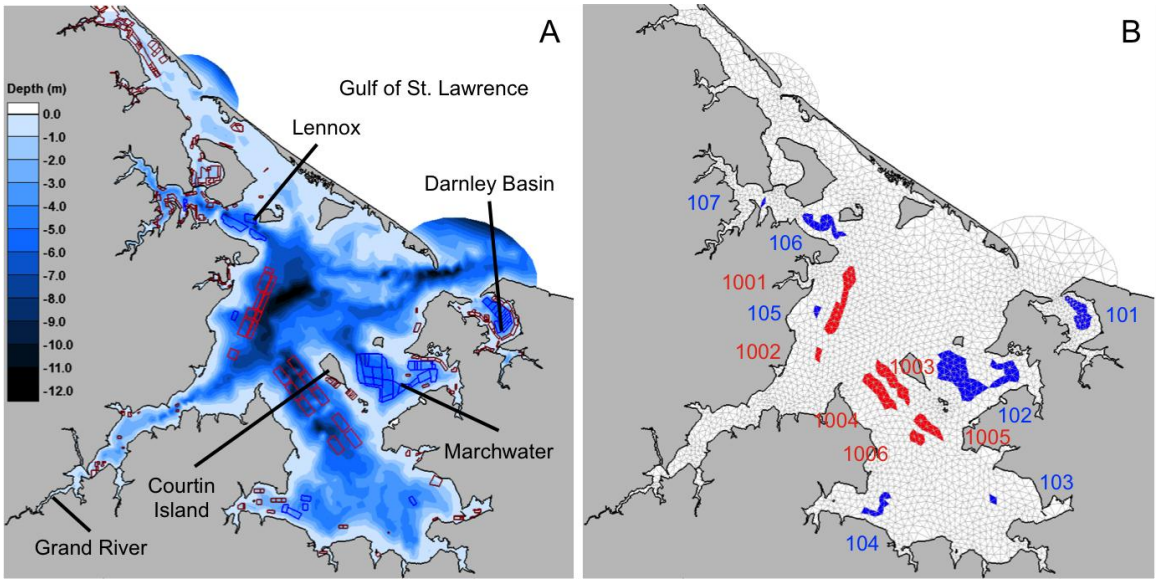

Figure 2. Transfer time and transfer rate between element #1004 (in red) and all other elements of the grid.

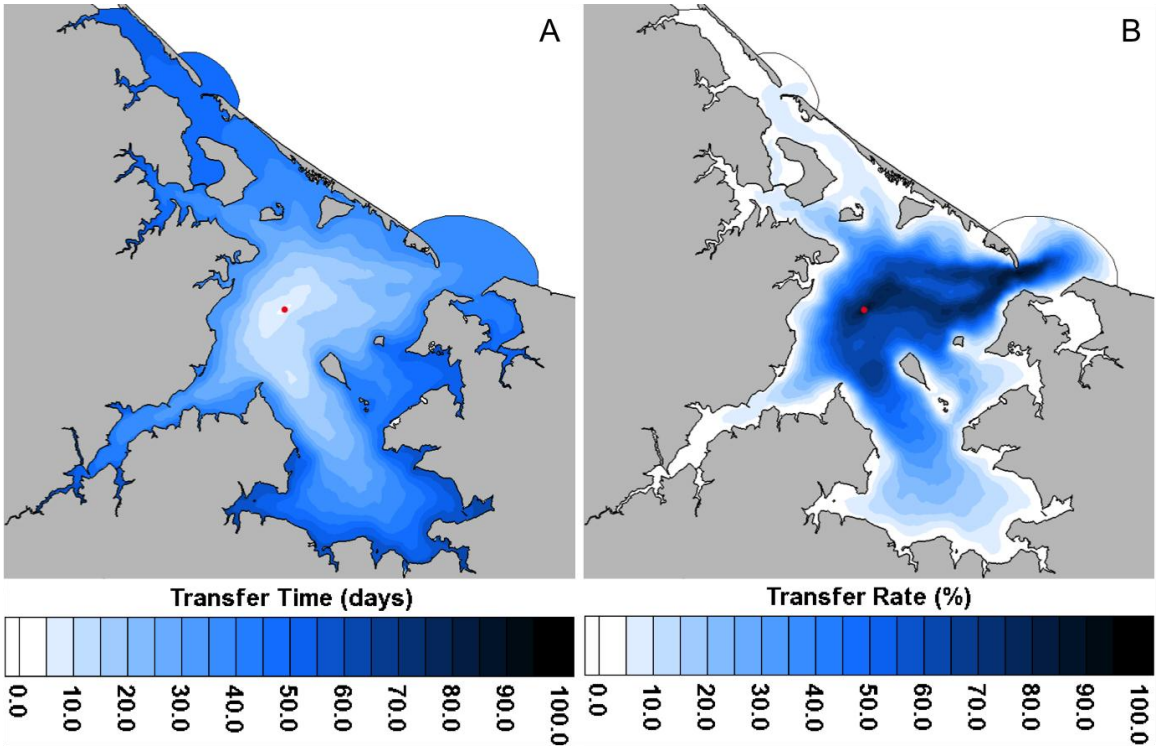

Figure 3. The most significant inter-lease connections from current to other leases (A) and from projected leases to other leases (B). These connections are identified in each panel for clarification.

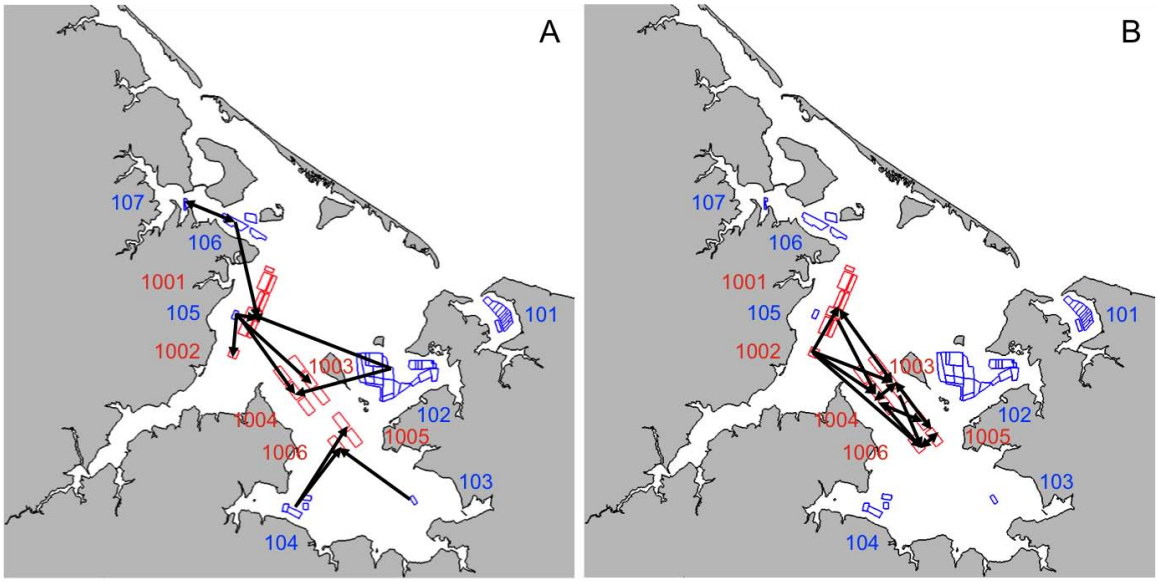

102 ➔ 1001, 1004
103 ➔ 1006
104 ➔ 1005, 1006
105 ➔ 1001, 1002, 1003, 1004
106 ➔ 107, 1001
107 ➔ 106

1001 ➔ 1002, 1003, 1004
1002 ➔ 1001, 1004, 1006
1003 ➔ 1001, 1004, 1005, 1006
1004 ➔ 1003, 1005, 1006
1005 ➔ 1003, 1004, 1006
1006 ➔ 1004, 1005

Figure 4. Seston Depletion Index (SDI, %) for current leases (A) and current leases plus projected leases (B).

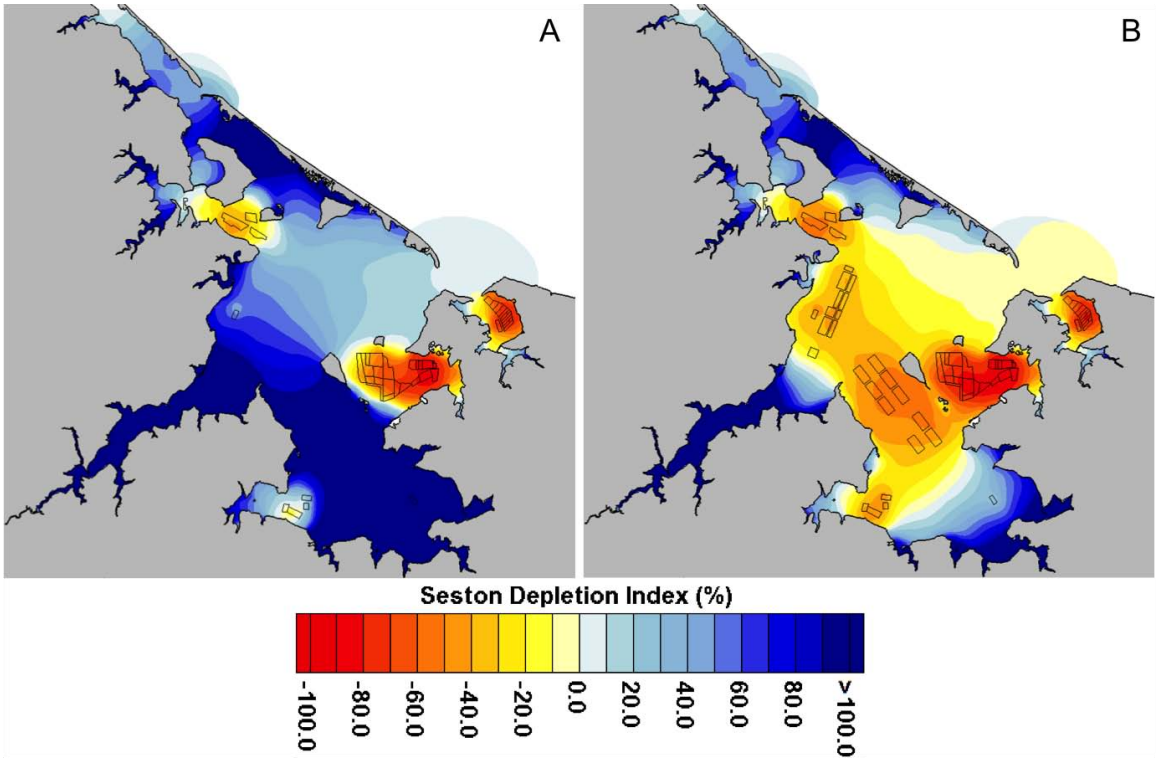

Figure 5. Absolute change in organic seston concentration in the projected scenario compared to the current scenario.

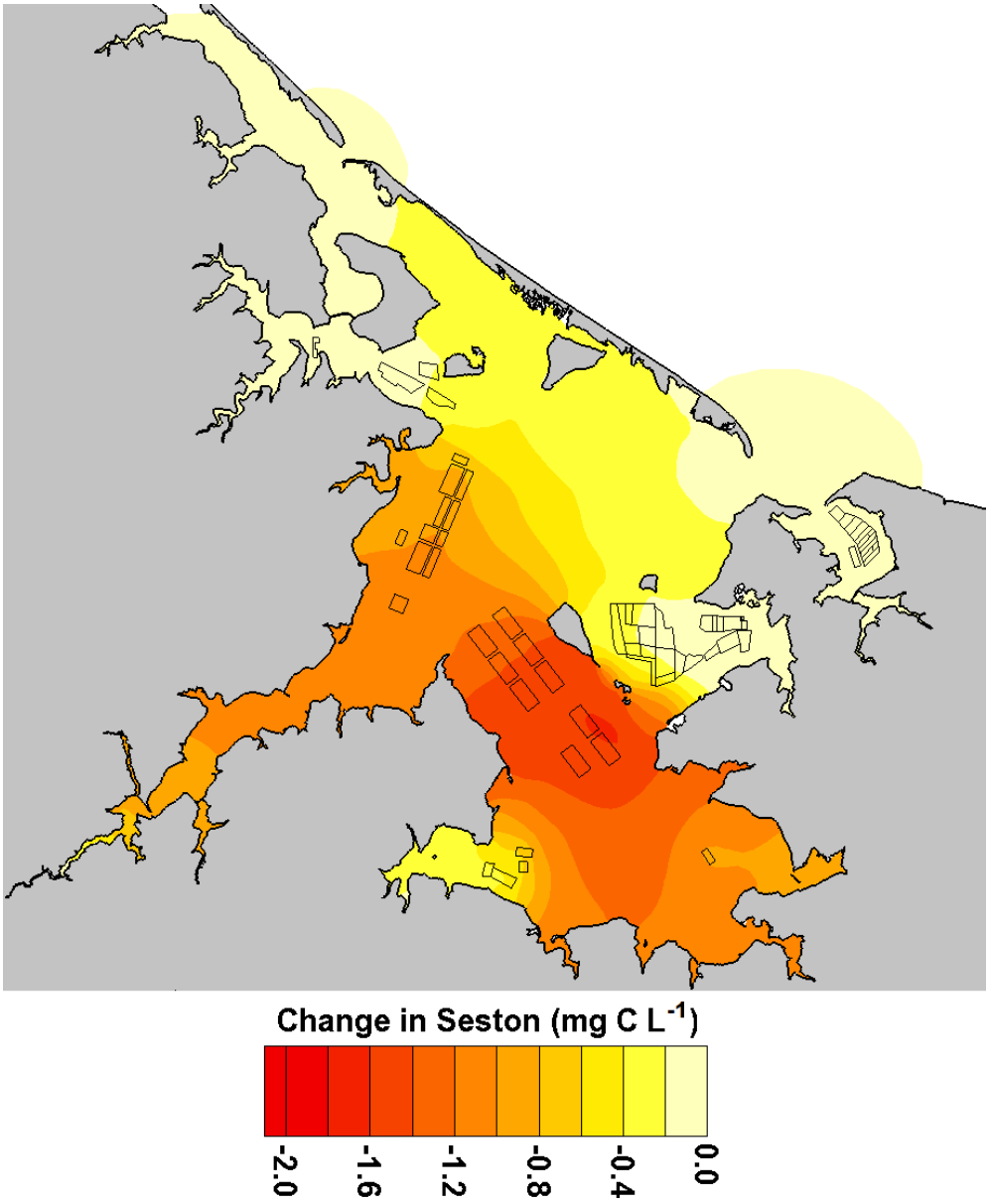

Figure 6. Phytoplankton Depletion Index (PDI, %) for current leases (A) and current leases plus projected leases (B).

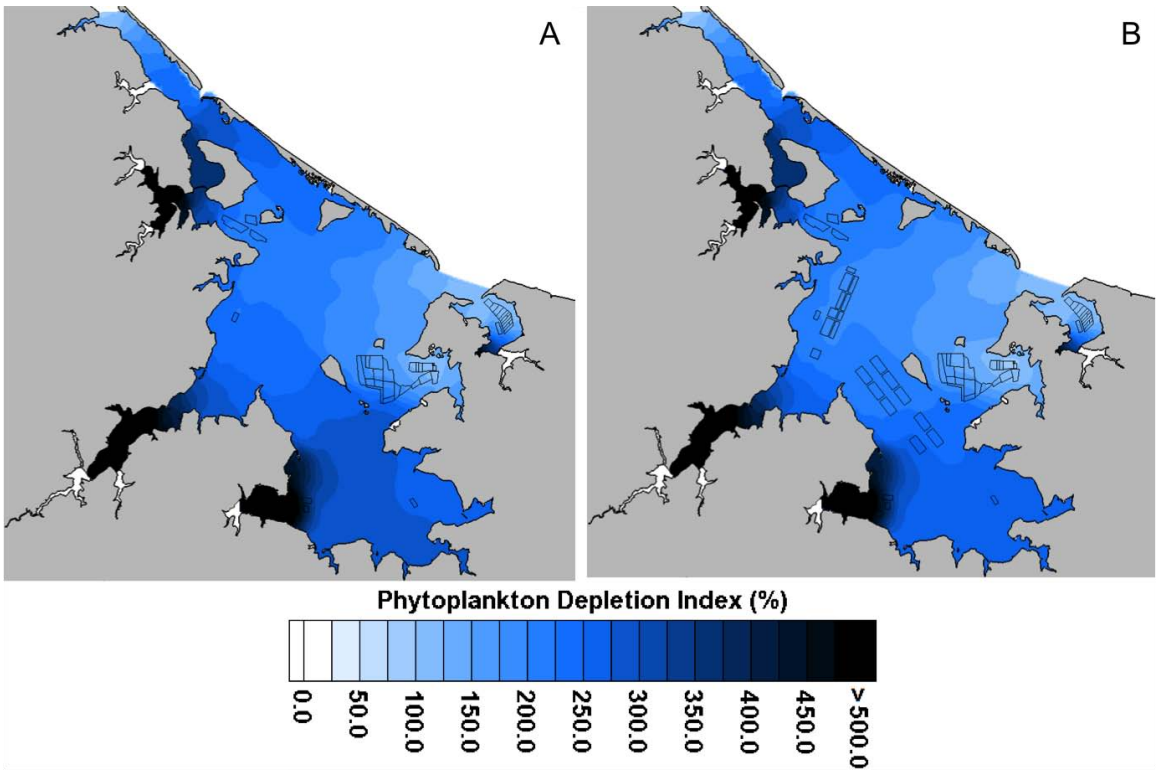

Figure 7. Absolute change in phytoplankton concentration in the projected scenario compared to the current scenario.

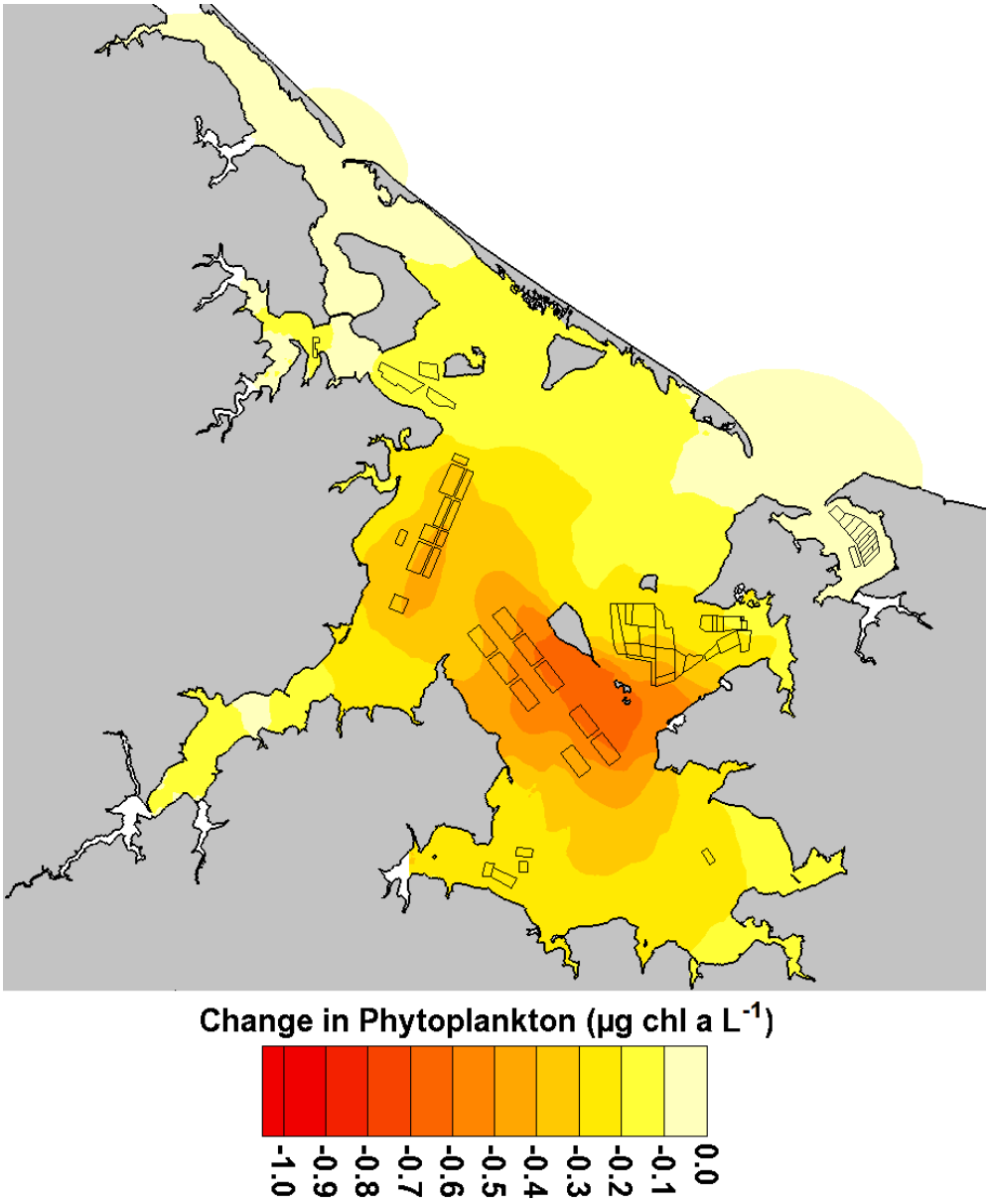

Figure 8. Absolute change in phytoplankton concentration in projected scenario (A) without leased areas #1005 and #1006, and (B) without leased area #1003, compared to the current scenario.

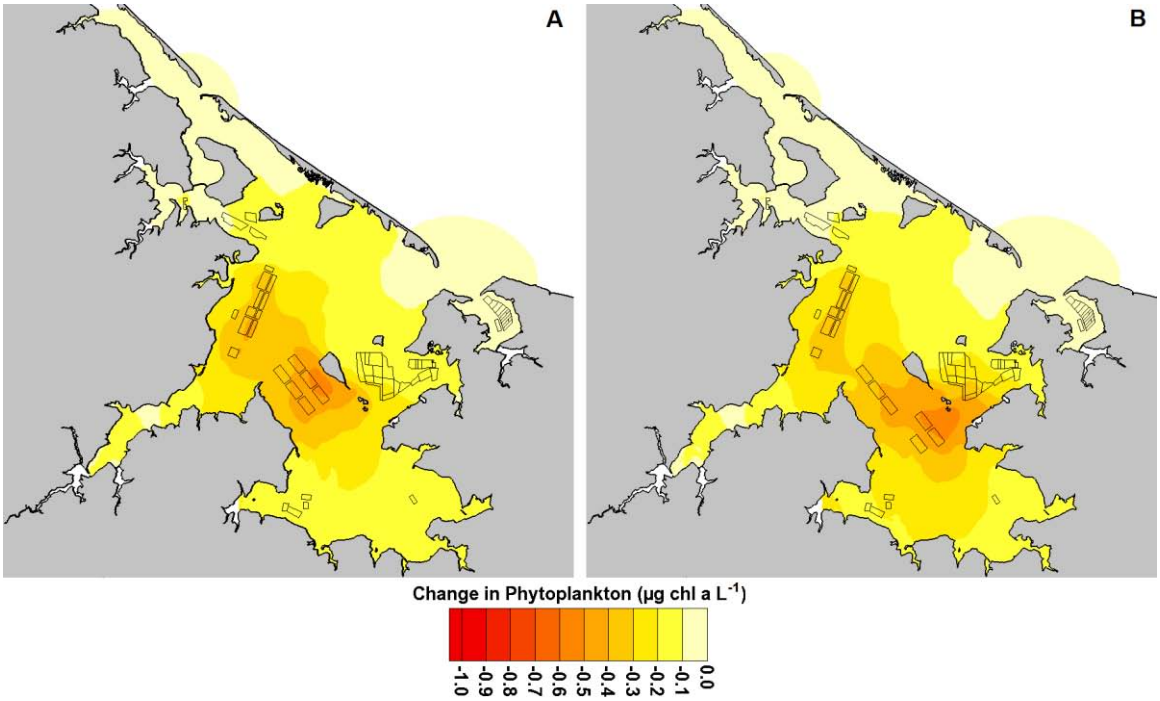

Appendix A. Available datasets for ecosystem model

The five largest rivers were considered in the current model. River flows were obtained from Environment Canada (http://www.ec.gc.ca). Nutrient time series in these rivers were generated using the Department of Environment, Labour and Justice of PEI database (http://www.gov.pe.ca/environment). Multi-year data were pooled together in order to generate continuous time series that represent average conditions in the different rivers. Given that there is no nutrient data available for River 5 (Figure A.1), the same values used for River 1 were used to force River 5 based on the similitude of land-use pattern of both watersheds.

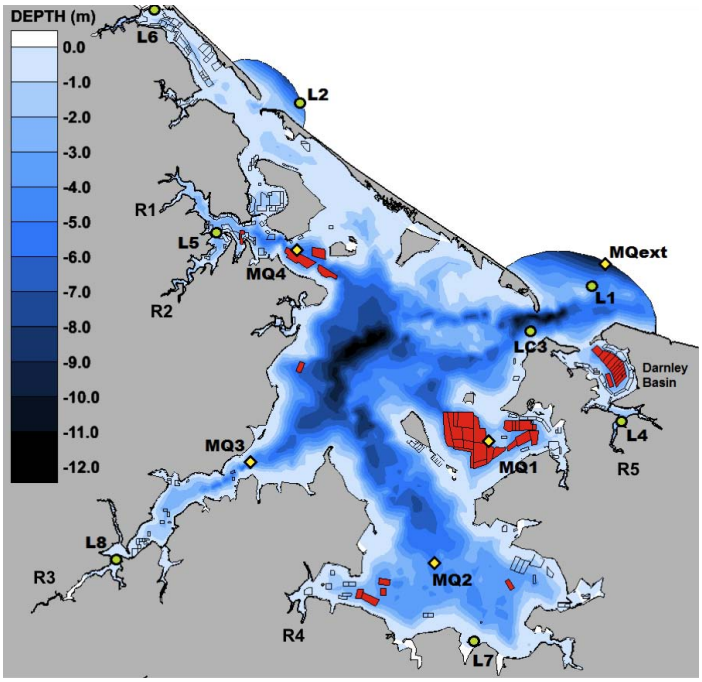

Figure A.1. Map of Malpeque, including bathymetry, current leases (red polygons), sampling stations (MQ1, MQ2, MQ3, MQ4 and MQext), rivers (R1, R2, R3, R4 and R5), and hydrodynamic stations (L1, L2, LC3, L4, L5, L6, L7 and L8. L = Water level. C = Current meter).

Monthly temperature, chlorophyll, seston and nutrient samples were collected from 24 May to 20 November 2012 at four stations inside the bay (MQ1 – MQ4) and one external station (MQext) that was used as a boundary condition (Figure A.1). Water samples for chlorophyll analyses were collected in duplicate. Samples were filtered through 25 mm Whatman GF/F filters, and then kept frozen (-20 ºC) until analysis, which was performed following EPA Method 445.0. Chlorophyll concentration was converted to carbon units assuming a carbon:chl of 50:1. Total Particulate Matter (TPM) was measured gravimetrically on pre-ashed (500 ºC, 4 h) 47 mm Whatman GF/F filters. Two replicates were collected at each sampling point. After filtering, the salts were eliminated by washing with isotonic solution of 0.5M ammonium formate. The filters were dried at 70 ºC for 24 h and weighed to determine the TPM. Particulate Organic Matter (POM) was determined after ashing the filters for 6 h at 500 ºC. The detrital carbon was calculated by multiplying the POM value by 0.5 and subtracting the phytoplankton carbon (Filgueira and Grant 2009). Pre-filtered water samples (syringe filters, 0.8 µm) were analysed in duplicate at each station for nutrient concentrations with a Seal Automatic Analyser III (SEAL Analytical Inc., Mequon, Wisconsin, USA) and following the colorimetric methods described by Strickland and Parsons (1972).

References

Filgueira R, Grant J (2009) A box model for ecosystem-level management of mussel culture carrying capacity in a coastal bay. Ecosystems 12:1222-1233

Strickland JDH, Parsons TR (1972) A practical handbook of seawater analysis. Fisheries research board of Canada, Vol 167

Appendix B. Hydrodynamic model

RMA-10 solves the Reynolds form of the Navier-Stokes equations for momentum, the continuity equation and a convection-diffusion equation for transport of heat, salinity and any dissolved or suspended matter. It uses a Smagorinsky scheme (Smagorinsky 1963) to estimate horizontal eddy diffusivities.

Sea level fluctuations forcing the hydrodynamic model were recorded using tide gauges (Water Level Data HOBO Logger, Onset Computer Corporation Inc. Bourne, MA, USA) at outside stations L1, L2 and L6 (Figure B.1). Inner stations (LC3, L4, L5, L7 and L8) shown on Figure B.1 were equipped with HOBO tide gauges and one of them (LC3) with a current meter (Workhorse Sentinel, Teledyne RD Instruments, Poway, CA, USA) and were used for validation purposes.

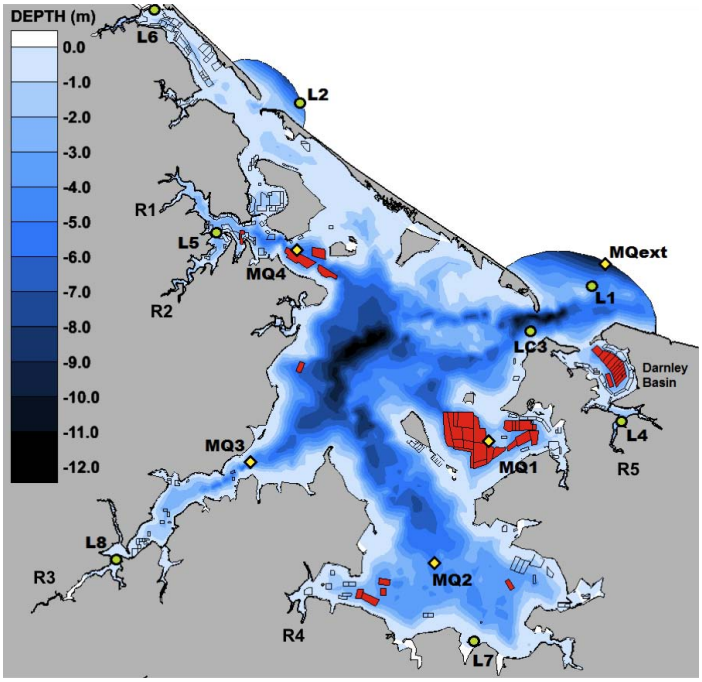

Figure B.1. Map of Malpeque, including bathymetry, current leases (red polygons), sampling stations (MQ1, MQ2, MQ3, MQ4 and MQext), rivers (R1, R2, R3, R4 and R5), and hydrodynamic stations (L1, L2, LC3, L4, L5, L6, L7 and L8. L = Water level. C = Current meter).

According to the different measures of goodness-of-fit reported in Table B.1, good agreement between observations and model results was reached for both currents along their principal axis (C3) and water levels all around Malpeque Bay. The normalized bias shows more discrepancy for water levels at stations L5 and L7. However, even at these stations model predictions lie within one standard deviation from observations which in absolute value translate to a mean model error < 4 cm. In particular, results of the harmonic analysis (Foreman 1977) of observed and predicted water level time series at all inner stations show that tidal propagation within the system is well reproduced by the model.

Table B.1. Harmonic analysis of observed and predicted water level time series with 95% confidence intervals for the three main tidal constituents (O1, K1 and M2) and fraction of the total variance of observed level fluctuations explained by the model at all sampled stations inside the domain.

	Amplitude (m)		Phase (°)			Amplitude (m)		Phase (°)	
	Observed	Predicted	Observed	Predicted		Observed	Predicted	Observed	Predicted
	O1					**K1**			
LC3	0.17 ± 0.05	0.17 ± 0.06	248.1 ± 13.0	240.1 ± 18.0	LC3	0.17 ± 0.05	0.15 ± 0.05	285.6 ± 17.2	278.6 ± 21.6
L4	0.16 ± 0.05	0.17 ± 0.04	262.6 ± 19.4	254.5 ± 16.9	L4	0.15 ± 0.05	0.16 ± 0.04	299.5 ± 21.3	293.1 ± 17.4
L5	0.17 ± 0.05	0.17 ± 0.05	249.8 ± 21.4	252.5 ± 19.4	L5	0.17 ± 0.06	0.17 ± 0.06	284.9 ± 22.7	292.1 ± 20.6
L7	0.17 ± 0.06	0.18 ± 0.06	251.5 ± 21.3	251.5 ± 19.4	L7	0.17 ± 0.07	0.16 ± 0.06	289.2 ± 19.9	294.2 ± 18.8
L8	0.17 ± 0.07	0.17 ± 0.06	254.7 ± 20.5	257.4 ± 15.3	L8	0.17 ± 0.06	0.16 ± 0.05	289.2 ± 24.3	300.3 ± 19.4
						Explained		**Normalized**	
	M2					**Variance (%)**		**Bias (%)**	
LC3	0.14 ± 0.04	0.15 ± 0.04	205.6 ± 14.1	195.6 ± 14.7	LC3	93.7		8.08	
L4	0.12 ± 0.04	0.12 ± 0.04	231.9 ± 14.7	213.3 ± 21.2	L4	84.2		8.12	
L5	0.18 ± 0.05	0.16 ± 0.04	217.0 ± 15.6	222.1 ± 13.3	L5	88.9		42.64	
L7	0.18 ± 0.04	0.17 ± 0.04	218.8 ± 15.0	220.1 ± 15.3	L7	89.5		-72.80	
L8	0.18 ± 0.05	0.16 ± 0.05	226.2 ± 16.3	232.8 ± 15.7	L8	77.0		0.78	
					C3	91.3		0.45	

$$Normalized\ Bias = 100 \times \frac{\overline{OBS} - \overline{PRED}}{\sigma_{OBS}}$$

where: $\overline{OBS}$ and $\overline{PRED}$ are the means of observations and model predictions, respectively

σ_{OBS} is the standard deviation of observations.

Predicted tidal circulation in Malpeque is presented in Figure B.2, both at a) maximum flood and b) maximum ebb currents. The inlets to the Gulf of Saint-Lawrence are the most dynamic areas with currents in excess of 1 m s^{-1}. The circulation remains fairly active over most of the central basin of the bay with maximum tidal currents of 10 – 15 cm s^{-1}, while inner parts of Darnley Basin, Marchwater and the south bay show much less water exchange with maximum currents reduced to a few cm s^{-1}.

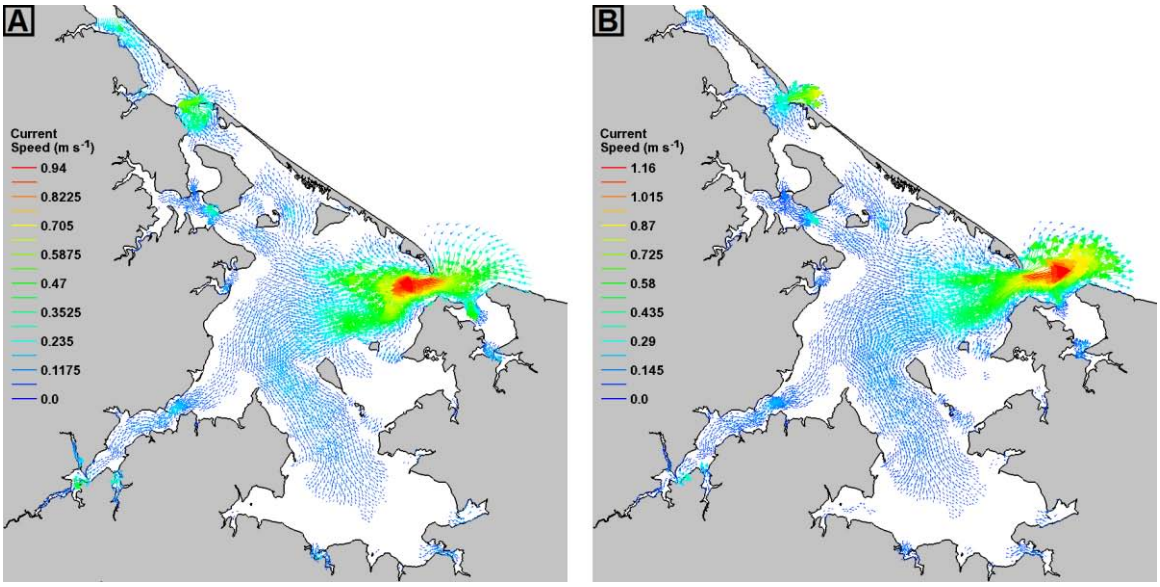

Figure B.2. Map of tidal currents predicted in Malpeque Bay at a) maximum flood and b) maximum ebb.

References

Foreman MG (1977) Manual for tidal heights analysis and previsions. Pacific Marine Science Report 77-10

Smagorinsky J (1963) General circulation experiment with the primitive equations. Mon Weather Rev 91: 99−164

Appendix C. Volumetric flow calculation (based on Filgueira et al. 2012).

Every node (vertex of each triangle) of the grid is represented with X and Y Cartesian coordinates. For each node, RMA provides values for three quantities at each time step: water speed in the x-direction, water speed in the y-direction and water depth. RMA stores the results in matrices that can be programmatically retrieved and manipulated. Each element (triangle) of an unstructured triangular grid can be surrounded by a maximum of 3 elements and a minimum of 1 element. The exchange of water for a given element is defined in relation to each of the surrounding elements in the grid in terms of volumetric exchange. The volumetric flow through a link from one element to another is calculated by multiplying the net velocity by the cross-sectional area through the side:

Volumetric Flow = (net velocity) x cross-sectional area
= (net velocity) x (average depth at the two nodes of the link) x (length of link)

The net velocity (nx.u+ny.v) is defined as the projection of the velocity vector (u, v) at the centre of each side (link) into the unit perpendicular vector of the link (nx, ny). The units of the velocity vector (u, v), where u is the average velocity in the x-direction at the two ends of the link and v is similarly defined for the y direction, are adjusted to meters per day. The unit perpendicular vector (nx, ny) is defined to point towards the centre of the element (Figure C.1a). Therefore a positive/negative net velocity indicates that flow is into/out of the element.

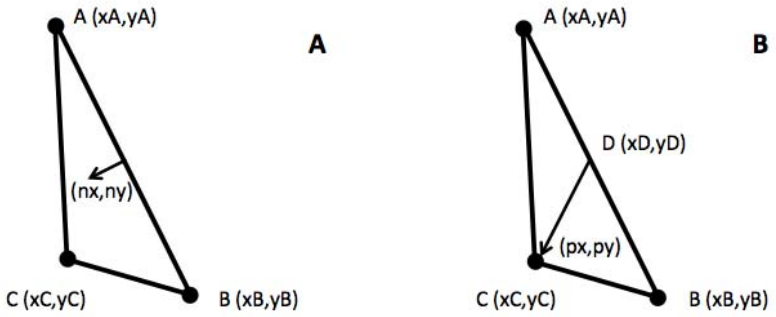

Figure C.1. Structure of the element defined by the nodes A (xA,yA), B (xB,yB) and C (xC,yC) and vectors used to calculate the flow through the link A-B. A. Vector (nx, ny) originates at the bisection of link A-B and is oriented perpendicular to A-B. B. Vector (px,py) originates at the bisection of the link A-B, D (xD,yD), and is directed to the node that opposes A-B, C (xC,yC).

Taking into account the node coordinates (xA, yA) and (xB, yB), the (nx, ny) vector is calculated as follows (Figure C.1a):

$nx = -(yA-yB)/[(xA-xB)^2+(yA-yB)^2]^{0.5}$
$ny = (xA-xB)/[(xA-xB)^2+(yA-yB)^2]^{0.5}$
or
$nx = (yA-yB)/[(xA-xB)^2+(yA-yB)^2]^{0.5}$
$ny = -(xA-xB)/[((xA-xB)^2+(yA-yB)^2]^{0.5}$

In order to compute which of the vectors is directed into the element, the (nx, ny) vector must be compared with the direction of the vector (px, py) whose origin is the bisector of the link and whose terminus is the opposing node (Figure C.1b). If the quantity nx.px+ny.py is positive, (nx, ny) and (px, py) follow the same direction into the element, and vice versa for negative values.

RMA provides a time series for water velocity and depth at each node, and the protocol described above can be applied to each time step. The volumetric flows for all time steps are averaged as a daily average for each link following a first order upwind scheme. The error of this scheme is kept to a minimum if the spatial and temporal variation of the concentration of a conservative tracer remains small for each element and time step:

$$Error_{spatial}\ (\%) = \left(\frac{|\Delta \mathrm{Conc.}|}{\overline{Conc.}}\right)^2_{spatial} \times 100 \qquad Eq.C.1$$

$$Error_{time}\ (\%) = \left(\frac{|\Delta \mathrm{Conc.}|}{\overline{Conc.}}\right)^2_{time} \times 100 \qquad Eq.C.2$$

where $|\Delta Conc.|$ is the absolute difference in concentration between two connected elements at a given time (Eq. C.1), or between two time steps for the same cell (Eq. C.2). $\overline{Conc.}$ is the mean concentration of both values for each case. The calculation of this error is crucial for evaluating the general error of the coupling scheme.

The numerical procedure carried out to calculate the exchange and the averaging process can produce a residual water imbalance within the bay. A minimization algorithm under constraint (pinv function in Matlab) was applied to the averaged exchange in order to minimize this water imbalance (to make the net flows zero) while keeping the correction factors as small as possible. After this process, the averaged volume (m^3) of each element and the averaged volumetric exchange rates (d^{-1}) for each link, i.e between every adjacent element pair, are used to define the average circulation of the bay (Filgueira et al. 2012).

References

Filgueira R, Grant J, Bacher C, Carreau M (2012) A physical-biogeochemical coupling scheme for modeling marine coastal ecosystems. Ecol Inform 7:71-80